Structural and Multidisciplinary Optimization (2020) 61:2271–2289
https://doi.org/10.1007/s00158-019-02481-7

RESEARCH PAPER

Topology optimization for periodic multi-component structures with stiffness and frequency criteria

Simon Thomas[1] · Qing Li[1] · Grant Steven[1]

Received: 15 September 2019 / Revised: 29 November 2019 / Accepted: 12 December 2019 / Published online: 20 February 2020

Abstract

Design of engineering structures may benefit from reduction in assembly complexity through use of periodic components, in which uniform sub-structures combine to form a relatively simple topology. The benefits of periodic structures include lower manufacture costs as well as ease of assembly. Recent developments in periodic topology optimization have shown its efficacy for addressing a range of design objectives. However, constraints such as assembly conditions and the connection configuration of periodic sub-components present limiting factors in the application of periodic optimization to real-world engineering problems. This study addresses the current knowledge gap in periodic optimization assembly through inclusion of common interfacing connections between periodic components, such as screws, welds, or rivets, thus accounting for real assembly conditions. A bi-directional evolutionary structural optimization (BESO) method and solid isotropic material with penalization (SIMP) method are presented, for stiffness and frequency criteria, which simultaneously optimizes the topology of the periodic components and the joint configuration connecting components. Elemental sensitivities are derived and utilized to drive the design of both the periodic component and the connection layouts. Iterative updating of the topological design, guided by elemental sensitivities, allows for optimization of the periodic topology for given objective functions. To demonstrate the effectiveness of the proposed method, optimized structures are explored through different periodicities. Application of the methodology presented in this study will assist in providing new design capabilities to reduce the costs of manufacturing, transport, and assembly through optimized periodic components.

Keywords Multi-component connection layout · Periodic structures · Topology optimization · Stiffness · Frequency

1 Introduction

Topology optimization aims to find the optimal layout of material within a given design domain to maximize desired performance such as stiffness, natural frequency, conduction, buckling, or a combination thereof (Bendsøe 2009).

Topology optimization has emerged as a field of study greatly impacting industry over recent years, in which numerous effective approaches have been developed and validated. These include homogenization (Bendsøe and Kikuchi 1988; Ma et al. 1993; Hassani and Hinton 1998), solid isotropic material with penalization (SIMP) (Bendsøe and Sigmund 1999; Sigmund 2001; Tcherniak 2002), evolutionary structural optimization (ESO) (Xie and Steven 1993, 1994, 1996, 1997; Yang et al. 1999; Rong et al. 2000; Huang and Xie 2010), and level set methods (Wang et al. 2003; Allaire et al. 2004; Shu et al. 2011). Topology optimization algorithms generally fall into the categories of density method or boundary method. The density method encompasses the homogenization, SIMP, and ESO methodologies while the boundary method was developed more recently and involves algorithms such as the level set method. Each of the different methods provides their own benefits to applications of topology optimization in different areas (Rozvany 2009; Huang and Xie 2010; Sigmund and Maute 2013; van Dijk et al. 2013; Xia et al. 2018).

Responsible Editor: Emilio Carlos Nelli Silva

✉ Simon Thomas
stho1573@uni.sydney.edu.au

Qing Li
qing.li@sydney.edu.au

Grant Steven
grant.steven@sydney.edu.au

[1] School of Aerospace, Mechanical and Mechatronic Engineering, The University of Sydney, Sydney, New South Wales, Australia

The SIMP algorithm discretizes a design domain into finite elements where the relative density of each element becomes the design variables of the optimization problem. The material properties follow a power law scheme, penalizing intermediate density elements and driving the topology to an optimized binary state of solid and void material (Bendsøe and Sigmund 1999; Sigmund 2001; Tcherniak 2002). ESO operates similarly to SIMP; however, binary element states are enforced as either solid or void material. In the original formulations of ESO, void material was wholly removed from the FEA model, known as hard kill, which prompted criticism due to potential of highly non-optimal solutions (Zhou and Rozvany 2001; Rozvany 2009). A soft-kill BESO variant was subsequently developed, which utilizes the SIMP power law, allowing void elements to be retained within the mesh. It may then be said that soft-kill BESO is a special case of standard SIMP, with discretely updated density states (Huang and Xie 2010). There exists ongoing debate as to the optimal application of BESO and its relation to other topology optimization algorithms (Munk et al. 2017; Huang and Xie 2010; Xia et al. 2018). The Level set method forms structural boundaries through a higher-dimensional scalar function, in which the "level" of the function is "set" such that the topological boundary is represented by the iso-contours of the Level set function which may be updated by Hamilton-Jacobi equations (Wang et al. 2003; Allaire et al. 2004; Shu et al. 2011; van Dijk et al. 2013).

The application of topology optimization optimization algorithms to real-world problems has been somewhat hindered due to the focus of most current literature on single component structures (Bendsøe 2009; Sigmund and Maute 2013; Xia et al. 2018). However, most engineering structures comprise of multiple sub-components, which at a structural level are connected via an interfacing such as adhesive, screws, welds, or rivets. Layout of such interfacing elements must be incorporated with topology optimization of individual sub-components to ensure desirable performance of multi-component systems. While some preliminary work for multi-component optimization has been carried out, it is under-studied in comparison with optimization for single components (Li et al. 2001b; Zhu et al. 2016).

Some engineering structures require large components and often exhibit complex material layouts which results in high manufacturing, transport, and installation costs. An appealing way to deal with such an engineering issue is to use multiple identical sub-components which are small relative to the design domain, and thus more easily manufactured and transported. Topology optimization of such repetitive sub-components, known as periodic optimization, enables compromise between system complexity and costs (Zhang and Sun 2006; Huang and Xie 2008; Zuo 2009; Chen et al. 2010; Xie et al. 2012), which is particularly attractive in mass-production and simplicity of assembly.

A key issue inhibiting the widespread application of topology optimization is the difficulty in transition between optimized designs and practical manufacturing. For instance, casting and extrusion production are two common fabrication methods, each of which exhibits significant complications when attempting to fabricate the complex designs produced by topology optimization processes (Zhou et al. 2002). Further research addressed manufacturing concerns from a milling and lithography perspective which may produce uniformly too thin or too thick components, with an extension to topology optimization methodology presented which was able to account for these manufacturing uncertainties with little decrease in system performance (Sigmund 2009; Schevenels et al. 2011). Length scale control is also a critical factor in machinability, preventing formations of small voids or intricate component sections, often addressable with appropriate filtering techniques (Sigmund and Petersson 1998; Sigmund 2007). Furthermore, cost of design may be included within the optimization process concurrently optimizing for performance and manufacturability (Liu and Ma 2015). A comprehensive review of component manufacturing limitations as related to topology optimization may be found in the reference material (Zhang et al. 2011; Liu and Ma 2016).

Multi-component optimization has drawn attention through different applications in literature, such as placements of fixture positions (Menassa and DeVries 1989, 1991), location of spot welds (Chirehdast and Jiang 1996), profile of adhesive bonding (Jiang and Chirehdast 1997), and configuration of discrete joint elements (Li et al. 2001b), which were largely based upon topology optimization techniques developed for single component structures (Chickermane and Gea 1997). Zhu et al. proposed to embed non-design sub-components within a macro-design domain (Zhu et al. 2017), enabling structural integration of small load-bearing components within a larger assembly, which exhibits significant advantages in design of complex structures (Qian and Ananthasuresh 2004). Zhang et al. adopted finite circle method to enforce non-overlap constraints between components to approximate a complex component through a set of circles with varying size and placement (Zhang et al. 2011). Liu and Kang explored the embedding field to address multi-component problems by modeling material interfaces between components, providing more realistic modeling of assembly conditions (Liu and Kang 2018). Note that placement of interfacing material such as screws, welds, or rivets may represent a special case of the embedding problem, where limited work is available to tackle such specific features (Qian and Ananthasuresh 2004). More recent work on multi-component optimization subdivided the structure into a multi-component assembly of bars (Hoang and Jang 2017; Wang et al. 2018), which are movable and morphable allowing them to approximately

conform to similar design achieved through classical single component optimization.

A significant feature of multi-component systems is structural periodicity, which refers to multiple identical substructures in a system. Periodic structures are widely used in engineering and architecture, some examples including, brick walling, tiling, trusses, bridge frames, and aircraft hulls. The pervasive use of periodicity is attributable to its simplicity of application and facilitation of cost reductions in manufacturing, assembly, and handling (Xie et al. 2011). Two key types of periodic topology optimization have been explored in literature: infinite periodicals and finite periodicals. The former has drawn much more extensive attention through an inverse homogenization procedure (Sigmund 1994), whereas the latter received relatively less attention. The fundamental difference between the two approaches resides in the scale of the structures considered. Infinite periodicals rely upon the presumption of repeating boundary conditions of each unit cell, allowing the FEA to be conducted in a unit cell domain. This has been commonly seen in microstructural design for materials, such as bone-lattice or honeycomb core of sandwich structures (Sigmund 1994; Hassani and Hinton 1998; Rodrigues et al. 2002). On the other hand, finite periodic structures do not necessarily exhibit repeating boundary conditions across unit cells. The lack of uniformity in structural behavior of each unit cell substantially increases the complexity of the topology optimization problem, as the entire structure must be modeled rather than reduction to a single unit cell. Alternatively, the macro-structure design domain is divided into a finite series of unit cells, exhibiting a specific type of periodicity such as translational, cyclic, or reflectional, as seen in Fig. 1 with the white square indicating the same periodic element within each of the iterated unit-cells. An example of 2D translational periodicity is the subdivision of a rectangular design domain into an m *by* n set of cells (a 1 *by* 1 representing typical single component design) with each unit cell exhibiting an identical design. In spite of its importance, there has been limited work available on finite periodic topology optimization to date, with most focusing on stiffness criteria (Zhang and Sun 2006; Huang and Xie 2008; Xie et al. 2012) and some extending to frequency and conductivity criteria (Zuo 2009; Chen et al. 2010).

It should be noted that the nature of finite periodic optimization consists of a trade-off between structural simplicity and structural performance. A fully optimized single cell topology may exhibit a relatively sophisticated configuration, thereby requiring higher manufacturing costs, although highly efficient, while a periodically optimized topology of unit cells may be simpler to manufacture and transport yet less efficient due to the inclusion of material in the unit cell design which is efficient in some, but not all, periodic cell locations within the macro-topology (Zhang and Sun 2006; Huang and Xie 2008; Chen et al. 2010).

1.1 Problem statement

A significant knowledge gap exists in current literature preventing the widespread adoption of topology optimization in the commercial engineering industry. Standard topology optimization is a useful and effective methodology for optimization of single components while existing multi-component optimization has been shown effective in allocation of interfacing material and periodic optimization is a proposed cost-effective method for industry applications. In literature, however, coupled topology optimization of realistic connection and periodic multi-components remains an open research question. This study aims to explore the knowledge gap between the three aforementioned topology optimization approaches through the presentation of a unified multi-component periodic topology optimization approach. The underlying method is applicable to many different objective functions and topology optimization algorithms but is explicitly be examined herein for stiffness and frequency criteria utilizing BESO and SIMP methodology. The study is expected to provide a method for production of cost efficient and multi-criteria designs, facilitating better manufacturability, transportability, and replicability in real engineering practice.

2 Multi-component modeling

Components within multi-component assemblies are mechanically or chemically bonded. At a structural level, this bonding exists as a material interfacing in the overlapping

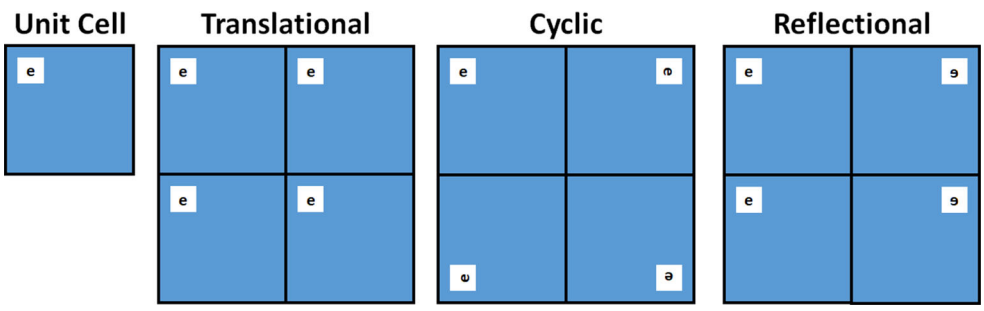

Fig. 1 Periodicity examples

regions between two components. Typical bonding methods include screws, welds, rivets, adhesives, and clamps. The design and placement of this interfacing material may be subject to realistic manufacturing constraints such as the size of machinery, the discrete size of the utilized joint, and a minimum assembly spacing (Li et al. 2001b). A simple example of this premise is the space requirement of a screwhead around the screw-shaft, requiring a minimum separation between two neighboring screw joints. Often, interfacing regions between components only require a small fraction of the region to be populated, with joint material, to satisfy mechanical requirements. The design engineer may then wish to optimally place these joints to minimize the requisite amount of connective material and improve system performance.

2.1 Joint discretization and component meshing

The connection interface region between two components may be discretized into an array of potential joint locations, accounting for the manufacturing limitations of the intended joint type, which often come in standardized sizes and materials. Consider an overlapping region between two plates of dimensions x *by* y connected via rivets of a given diameter D, separated by a manufacturing spacing of Δ_c, as seen in Fig. 2. A simple M *by* N fixed grid mesh may be utilized to model the interface region, and joints may be approximately modeled through an m *by* n set of elements corresponding to the geometric size of the intended joint type D, while a specified gap Δ_c^e of void elements may then buffer each discrete joint location relative to the governing manufacturing constraints Δ_c. An example of this meshing procedure may be seen in Fig. 2.

The fixed grid mesh utilized in the interface region must also match the overlapping region of each of the components to allow for seamless meshing of the full structure. The simplest approach is to utilize a fixed grid mesh for each component, the sizing of which is governed by the discretized interface region. Due to the subdivision of a continuum structure into discrete elements of a limited mesh density, some degree of approximation in the meshing allocation is required to simultaneously model the joint sizing, gap sizing, and component sizing with an integer number of fixed grid elements. An appropriate meshing may be specified on a case by case basis dependent on intended joint type, spacing requirements, and component geometry. The multi-component topology optimization process is designed to allocate an optimal distribution of joints and thus the simplification of joint modeling may be justified. Application of topology optimization methods, such as SIMP and BESO, may selectively trend the distribution of joint material over successive iterations, as guided by the sensitivity analysis. A final design may then be produced with more rigorous modeling methods, which extrapolates the optimal rivet locations from the optimized model. An illustrative example of this process is seen in Fig. 3 for a theoretical component interface within a mechanical system.

3 Sensitivity analysis

The BESO and SIMP algorithms utilized throughout this study are driven by a topological sensitivity analysis. The sensitivity for each element is derived from finite element formulation by quantifying the influence of each element on a specific objective function. The sensitivity pattern subsequently guides the inclusion and exclusion of material in the next design iteration. The topological design is trended towards an optimum state over successive iterations subject to given design constraints, such as volume fraction. The derivation of sensitivities for a wide variety of multi-physical and multi-functional optimization criteria is possible (Yang et al. 1999; Li et al. 1999; Huang et al. 2010; Sigmund and Maute 2013); however, the examples in this study will be limited to stiffness and frequency criteria, the mathematics of which is briefly discussed in the following sections.

3.1 Stiffness criterion

The static equilibrium condition allows calculation of nodal displacements within the finite element model as a result of an applied load, as

$$\{\mathbf{f}\} = [\mathbf{K}]\{\mathbf{u}\} \tag{1}$$

where $\{\mathbf{f}\}$ is the global force vector, $[\mathbf{K}]$ is the global stiffness matrix, and $\{\mathbf{u}\}$ is the global nodal displacement

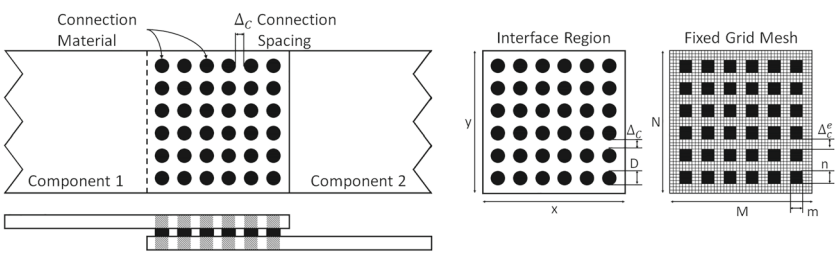

Fig. 2 Example connection interface discretization

vector (Cook and et al 2007). The stiffness of the structure may then be related to the inverse of the mean compliance C, the total strain energy from the applied load seen in (2). Stiffness optimization may be considered as a minimization of mean compliance for a given volume criterion (Huang and Xie 2010).

$$C = \frac{1}{2}\mathbf{f^T u} \tag{2}$$

Application of a material interpolation scheme allows for elements within the finite model to exhibit variable material properties, as governed by a power law as,

$$\rho_i = \rho_0 x_i, \qquad E_i = E_0 x_i^p, \qquad \nu_i = \nu_0 \tag{3}$$

where x_i is the relative density of the $i-th$ element; ρ_i, E_i, and ν_i are the elemental density, Young's modulus and Poisson's ratio, respectively; ρ_0, E_0, and ν_0 are the properties of the solid material, and p is a penalty factor (Bendsøe and Sigmund 1999; Sigmund 2001). The relative density x_i may be assigned a value from x_{min} to 1, and the penalty factor is commonly set to $p = 3$, while the minimum relative density often takes on a small value such as $x_{min} = 0.001$ (Huang and Xie 2010).

The change in mean compliance with respect to the change in elemental relative density may be quantified and utilized as an elemental sensitivity α_i^e, as,

$$\alpha_i^e = \frac{\partial C}{\partial x_i} = -\frac{1}{2}x_i^{p-1}\{\mathbf{u_i^e}\}^T[\mathbf{K_i^e}]\{\mathbf{u_i^e}\} \tag{4}$$

where $\{\mathbf{u_i^e}\}$ is the elemental nodal displacement vector and $[\mathbf{K_i^e}]$ is the elemental stiffness matrix of the $i-th$ element when solid ($x_i = 1$) (Xie and Steven 1997; Sigmund 2001; Huang and Xie 2010).

3.2 Frequency criterion

The dynamic behavior of a structure may be modeled through use of an eigen-value problem, as,

$$([\mathbf{K}] - \omega_j^2[\mathbf{M}])\{\mathbf{u_j}\} = 0 \tag{5}$$

where $[\mathbf{K}]$ is the global stiffness matrix, $[\mathbf{M}]$ is the global mass matrix, and ω_j is the $j-th$ natural frequency with $\{\mathbf{u_j}\}$ being the corresponding eigen-vector (Huang and Xie 2010). The Rayleigh quotient, seen in (6), links the eigen-vectors with their corresponding natural frequencies (Xie and Steven 1996).

$$\omega_j^2 = \frac{k_j}{m_j}, \quad k_j = \{\mathbf{u_j}\}^T[\mathbf{K}]\{\mathbf{u_j}\}, \quad m_j = \{\mathbf{u_j}\}^T[\mathbf{M}]\{\mathbf{u_i}\} \tag{6}$$

An alternative implementation of the material interpolation scheme, seen in (7), may be introduced for frequency analysis which helps prevent the manifestation of artificial localized modes of vibration within low density regions of the model which exhibit very large mass to stiffness ratios (Pedersen 2000).

$$\rho_i = \rho_0 x_i, \quad \nu_i = \nu_0,$$
$$E_i = E_0 * \left((x_{min} - x_{min}^p)/\left(1 - x_{min}^p\right)\left(1 - x_i^{(p-1)}\right) + x_i^p \right) \tag{7}$$

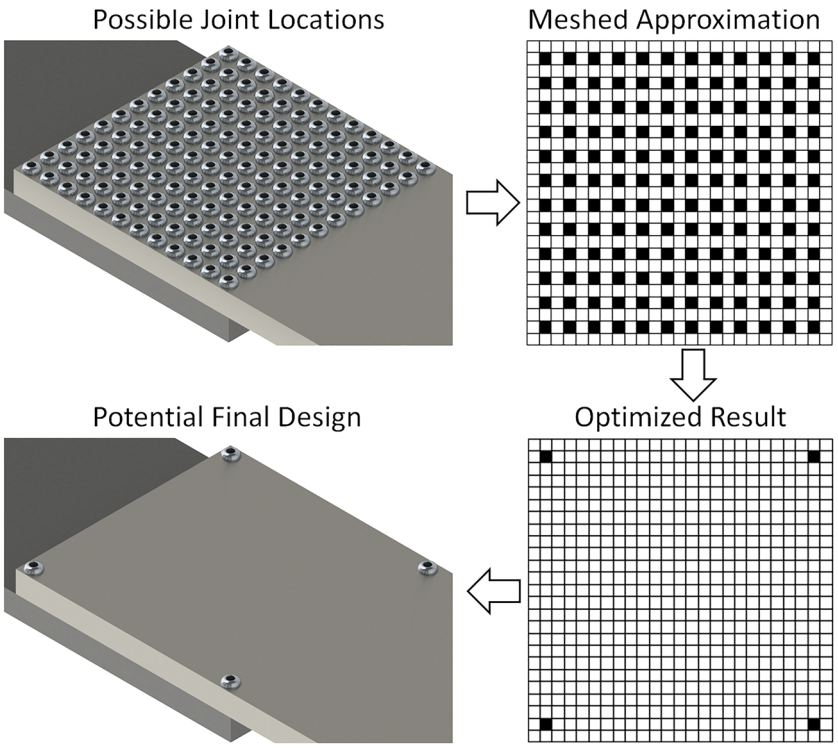

Fig. 3 Illustrative example of interface optimization process

The change in the $j-th$ natural frequency ω_j with respect to the change in elemental relative density x_i of the $i-th$ element may be quantified and utilized as a modal sensitivity α_{ij}^e, as,

$$\alpha_{ij}^e = \frac{\partial \omega_j}{\partial x_i} = \frac{1}{2\omega_j}\{\mathbf{u_{ij}}\}^T \left(\frac{1-x_{min}}{1-x_{min}^p} p x_i^{p-1} [\mathbf{K_i^e}] - \omega_j^2 [\mathbf{M_i^e}] \right) \times \{\mathbf{u_{ij}}\} \tag{8}$$

where $\{\mathbf{u_{ij}}\}$ is the elemental modal eigen-vector and $[\mathbf{K_i^e}]$ and $[\mathbf{M_i^e}]$ are the elemental stiffness and mass matrices respectively of the $i-th$ element when solid ($x_i = 1$). The modal eigen-vector $\{\mathbf{u_j}\}$ must be normalized with respect to $[\mathbf{M}]$. An elemental sensitivity may then be formed as a weighted average of each of the modal sensitivities α_{ij}^e, as

$$\alpha_i^e = \frac{\sum_{j=1}^N w_j \alpha_{ij}^e}{N} \tag{9}$$

where w_j is a weighting factor for the $j-th$ mode and N is the total number of modes in the objective function. The weighting factors may be prescribed values from -1 to 1, indicating the degree of maximization or minimization of a given natural frequency as determined from the respective frequency objective function.

3.3 Multi-criteria sensitivity

A multi-criteria sensitivity α_{mc}^e may be formulated by combining the sensitivities from different design criteria, specifically mean compliance and natural frequency in this study. The sensitivities may be calculated using a linear weighting function as seen in (10), where w is a weighting factor from 0 to 1, α_c^e are the compliance sensitives and α_f^e are the frequency sensitivities.

$$\alpha_{mc}^e = w\frac{\alpha_c^e}{|\alpha_c^e|_{max}} + (1-w)\frac{\alpha_f^e}{|\alpha_f^e|_{max}} \tag{10}$$

4 Topology optimization procedures

The underlying methodology of multi-component periodic topology optimization is independent of the update process utilized to drive the topological design. This study presents results utilizing BESO and SIMP; a brief discussion of each method is included below (Sigmund and Maute 2013; Huang and Xie 2010).

4.1 Mesh independent filter

Direct use of elemental sensitives obtained from low-order elements may lead to checkerboard patterns, producing unrealistic designs (Bendsøe and Sigmund 1995). This issue can be alleviated through application of a mesh independence filter, of which several variations have been presented (Sigmund and Petersson 1998; Li et al. 2001a; Bourdin 2001; Huang and Xie 2007).

4.1.1 BESO filtration

The BESO filtration scheme improves convergence and inhibits large fluctuation of the objective function (Huang and Xie 2007, 2010). It operates independently of the relative density of a given element, making it applicable to both soft- and hard-kill variations of BESO. Firstly, nodal sensitivities α_j^n are calculated from the elemental sensitivities α_i^e as,

$$\alpha_j^n = \sum_{i=1}^M w_i \alpha_i^e, \quad w_i = \frac{1-\frac{r_{ij}}{\sum_{i=1}^M r_{ij}}}{M-1}, \quad \sum_{i=1}^M w_i = 1 \tag{11}$$

where j is the considered node, M is the total number of elements connected to the $j-th$ node, and r_{ij} is the distance between the centroid of the $i-th$ element and the $j-th$ node. Secondly, the nodal sensitivities are re-distributed back to elemental sensitivities relative to a specified filter radius r_{min} as,

$$\widehat{\alpha_i^e} = \frac{\sum_{j=1}^N w(r_{ij})\alpha_j^n}{\sum_{j=1}^N w(r_{ij})}, \; w(r_{ij}) = r_{min} - r_{ij} \tag{12}$$

where the filtered elemental sensitivity $\widehat{\alpha_i^e}$ becomes a weighted average of nodal sensitivities α_j^n, where N is the total number of nodes within the specified radius from the centroid of the $i-th$ element. Finally, the filtered sensitivities are averaged with the historical sensitivities across the design iterations such that the sensitives are a composite of the previous sensitivity patterns, as,

$$\alpha_K = \frac{\widehat{\alpha^e} + \alpha_{K-1}}{2} \tag{13}$$

where K is the current iteration in the topology optimization process.

4.1.2 SIMP filtration

The SIMP filtration process is very similar to that of the BESO filter process; however, it avoids the use of nodal sensitives and includes the elemental relative densities in the algorithm (Sigmund and Petersson 1998; Sigmund 2001), as,

$$\widehat{\alpha_i^e} = \frac{1}{x_i \sum_{j=1}^N \widehat{H}_{ij}} \sum_{j=1}^n \widehat{H}_{ij} x_j \alpha_j^e, \quad \widehat{H}_{ij} = r_{min} - r_{ij} \tag{14}$$

where the $\widehat{H}_{ij}$ term is a convolution operator determined relative to the specified filter radius r_{min} and the distance r_{ij} from the centeroid of $i-th$ element from the centeroid of

the $j-th$ element, where N is the number of elements with a positive $\widehat{H}_{ij}$ value.

4.2 Periodic sensitivity

The topological update process relies upon the calculated elemental sensitivities to generate a new design. As the pertinent design of a periodic structure is the unit cell, the utilized sensitivities must be related to the unit cell. This is achieved through compression of a topology-wide sensitivity pattern to a unit cell sensitivity pattern, seen in Fig. 4. Specifically, through the calculation of an averaged elemental sensitivity α^e_{iuc} from the corresponding sensitivities of each iterated unit cell within the macro-structure, as,

$$\alpha^e_{iuc} = \frac{\sum_{k=1}^{U} \widehat{\alpha^e_{ik}}}{U} \tag{15}$$

where α^e_{ik} is the sensitivity of the $i-th$ corresponding element in the $k-th$ iterated unit cell and U is the total number of iterated unit cells. In this way, the structure-wide sensitivity is compressed into a periodic sensitivity for topological design of the recurring unit cells.

4.3 Optimization algorithms

BESO and SIMP utilize the filtered sensitivities to drive topological variation within the design domain in an iterative process, progressively morphing the structural topology towards an optimum (Huang and Xie 2010; Sigmund and Maute 2013). The design domain of the proposed periodic optimization algorithm is the unit cell, which utilizes the compressed filtered sensitivity pattern to update its design. The updated unit cell is then iterated to form the macro-structure, as seen in Fig. 4.

4.3.1 BESO update procedure

BESO iteratively updates the topology through assignment of either solid ($x = 1$) or void ($x = x_{min}$) status to corresponding elements within the design domain. In soft-kill, $x_{min} \approx 0.001$ and hard-kill $x_{min} = 0$. In the hard-kill scheme, void elements are entirely removed from the model, allowing for faster computational times, and may be considered a special case of the soft-kill method with a penalty factor tending towards infinity (Huang and Xie 2010).

At each design iteration, a new volume target is established (16), dictating the desired volume for the next iteration, relative to a prescribed evolutionary rate ER which is typically around 1% as,

$$\begin{aligned} V_K < V^* &: V_{K+1} = V_K(1+ER), \\ V_K > V^* &: V_{K+1} = V_K(1-ER) \end{aligned} \tag{16}$$

where the current volume V_K is compared with the volume criterion V^*, dictating the direction of volumetric movement. When the volume target is reached, the volume remains constant with equal material volume added and removed at each iteration (Huang and Xie 2010).

The application of a simple ruleset determines the void and solid status of each element in the next design iteration, seen in (17). The total solid volume must meet the next volume target V_{K+1} and a maximum addition ratio AR_{max} must not be exceeded, which is set by the user to limit oscillation between solid and void material. To drive the variation of elemental material status, an ordered ranking of elemental sensitives is assessed, from highest to lowest, and progressed through individually with a given element being solidified if its sensitivity rank satisfies the criterion, as,

$$V_{K+1} > V_{s\to s} + V_{v\to s}, \quad V_{K+1}AR_{max} > V_{v\to s} \tag{17}$$

where $V_{s\to s}$ is the total volume of solid to solid material to remain in its current status; $V_{v\to s}$ is the total volume to be changed from void to solid material. All the elements which fail the upgraded criterion are voided; once the maximum material addition limit is reached, all further void elements remain void regardless of their sensitivities. A similar procedure for BESO element updating may be found in the reference material (Huang and Xie 2010).

The BESO procedure may be terminated when one of two conditions is met, either once the total iterations

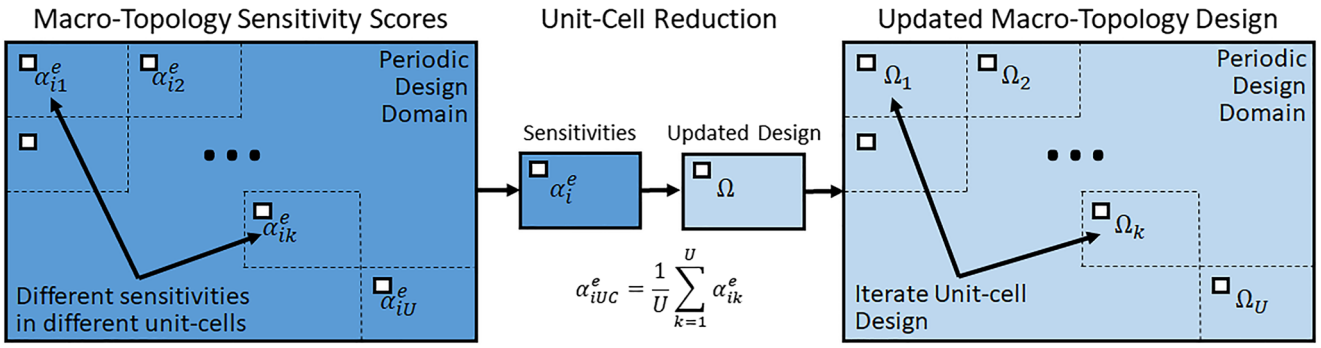

Fig. 4 Periodic sensitivity and synchronization of topology update

exceeds a prescribed iterative limit K_{max} or the fluctuations in the objective function f_K over recent iterations is less than a specified threshold τ while the volume criterion V^* is satisfied, mathematically as,

$$K > K_{max}, \quad or$$
$$V_k = V^* : \frac{|\sum_{i=1}^{N} f_{K-i+1} - \sum_{i=1}^{N} f_{K-N-i+1}|}{\sum_{i=1}^{N} f_{K-i+1}} \leq \tau \quad (18)$$

where K is the current iteration, V_K is the current volume, and $2N$ is number of considered recent iterations (Huang and Xie 2010). A criticism of the BESO algorithm involves the termination criterion, in which the topology may not be considered mathematically converged, as termination may occur despite ongoing changes to the topological design between iterations (Zhou and Rozvany 2001; Huang and Xie 2010; Sigmund and Maute 2013). Nevertheless, consideration of few last iteration results makes the termination more justifiable.

The elemental removal/voiding process functions slightly differently for connection interface BESO than in standard applications. Due to the discrete nature of joints, such as a single screw, the constituent elements within the mesh modeling a given joint location must be removed as whole units, a process known as grouped ESO (Lencus et al. 2002). The sensitivity score α_J for a given joint location may then be calculated as a weighted average of the constituent elemental sensitivities within the joint, as seen in (19), where N is the number of elements in the given joint, α_i^e is the elemental sensitivity, and v_i^e is the elemental volume. The joint locations with the lowest mean scores are then selected for removal.

$$\alpha_J = \frac{\sum_{i=1}^{N} \alpha_i^e v_i^e}{\sum_{i=1}^{N} v_i^e} \quad (19)$$

The bi-directional solution for ESO in single component optimization relies upon a continuous sensitivity distribution, allowing the natural expansion of the mesh in areas of high value. However, the spacing between joint locations may inhibit the accurate allocation of sensitivity scores to voided joint locations by the standard BESO filter, an issue especially prevalent at low material volumes with sparse joint patterns. Alternatively, the internal sensitivity distribution of a given joint location may be examined relating the centroid of sensitivity scores to the centroid of the joint location, thus producing a vector indicating the preferential direction of material addition/movement. This process may be seen in (20), where x_i^e and y_i^e are the elemental centroid coordinates and x_c and y_c are the joint centroid coordinates. Joint material may then be added, or an existing joint translated, to a voided joint location as directed by the sensitivity vector.

$$\mathbf{V} = V_x \mathbf{i} + V_y \mathbf{j},$$
$$V_x = \frac{\sum_{i=1}^{N} \alpha_i^e \left(x_i^e - x_c^j\right)}{N},$$
$$V_y = \frac{\sum_{i=1}^{N} \alpha_i^e \left(y_i^e - y_c^j\right)}{N} \quad (20)$$

A joint removal rate may be prescribed, removing an integer number of whole joints per iteration with the lowest mean sensitivity. Similarly, a joint addition rate may be set, allowing for up to a specified number of new joints to be added into vacant joint locations as indicated by the highest magnitude internal sensitivity vectors of the existing joints. Successive removal and addition of joints at low material volumes may result in the clumping of joint locations. To account for this issue, a volume addition threshold is set, under which no further joint additions are made. Alternatively, the joints with the highest magnitude vectors are translated to vacant neighboring locations, as indicated by the sensitivity vector, as opposed to a new neighboring joint being added. Removal of material continues until a specified volume criterion is met. Addition of material may occur above the volume addition threshold and translation of joints occurs under the volume addition threshold.

4.3.2 SIMP optimality criteria

The SIMP methodology assigns each element an updated relative density value x for the subsequent iteration of the optimization process relative to its sensitivity value. Intermediate density values are driven towards a binary result of x_{min} or 1 due to the penalization factor $p > 1$, typically with $p = 3$ the recommended value (Bendsøe and Sigmund 1999).

The topological design is driven via one of a variety of algorithms, including sequential linear programming (SLP), method of moving asymptotes (MMA) and the optimality criterion (OC) method (Sigmund and Maute 2013). For its simplicity, the OC procedure is adopted here as,

$$x_e^{new} = \begin{cases} max\,(x_{min}, x_e - m)\,, & if : x_e B_e^{\eta} \leq max\,(x_{min}, x_e - m) \\ x_e B_e^{\eta}, & if : max\,(x_{min}, x_e - m) < x_e B_e^{\eta} < min\,(1, x_e + m) \\ min\,(1, x_e + m)\,, & if : min\,(1, x_e + m) \leq x_e B_e^{\eta} \end{cases}$$
$$B_e = \frac{-\frac{\partial c}{\partial x_e}}{\lambda \frac{\partial V}{\partial x_e}} \quad (21)$$

where x_{min} is the minimum relative density, m is the move limit, η is the damping coefficient, λ is the Lagrangian multiplier, and V is the volume (Bendsøe and Sigmund 1995; Sigmund 2001). The filtered sensitivities compressed to a unit cell are used in this procedure.

The SIMP algorithm may be terminated once convergence is achieved or a maximum iteration limit is reached. As opposed to the BESO methodology which utilizes a convergence criterion based upon the stabilization of the objective function, the SIMP methodology may utilize a convergence criterion based upon the stabilization of the topological change, as,

$$\max_{i \in N_{uc}} \left| x_i^{new} - x_i^{old} \right| \leq \tau \tag{22}$$

where x_i^{new} and x_i^{old} are the updated and previous elemental relative densities, N_{uc} is the set of elements in the unit cell, and τ is the convergence threshold (Sigmund 2001).

As with the BESO method, a slight alteration to the standard SIMP procedure is required to apply topology optimization to the connection interface region. As joints must exist as whole units, each of the constitutive elements within a joint must exhibit the same material properties. In the SIMP algorithm, this requires each element within a joint location to exhibit the same relative density value. Updating of the joint interface is achieved through reduction of joint elements to a mean sensitivity value, as in (19), which is treated by the optimality criterion as a single element. Thus, updated relative density value of the joint describes the relative densities of all constituent joint elements. Joint values exhibiting intermediary relative density values in the converged model may be interpreted as joints of varying size.

5 Design examples

BESO is utilized as the primary algorithm for the generation of results due to its ease of application, clear binary outputs, and suitability for both compliance- and frequency-based criteria.

5.1 Cantilever structure

Topology optimization literature often utilizes benchmark case studies to illustrate the application of proposed algorithms. Single component topology optimization is often applied to a clamped cantilever beam with a lateral loading at the end of the beam (Huang and Xie 2010; Sigmund and Maute 2013; Xia et al. 2018). An example of the BESO process applied to this case study for a 60% volume constraint may be seen at the top of Fig. 5(a). The component's dimensions are 120 by 40 by $5mm$, made of steel with a $100N$ loading applied and a filter radius of $5mm$ meshed with 126 by 42 by 4 hexahedral elements. The resultant topological design exhibits a compliance of $0.74Nmm$ and may be smoothed for manufacture. Some degree of periodicity may be enforced on the cantilever structure, as may be seen in the second result set of Fig. 5(b) for a 2 by 1 periodic cantilever structure. The structural periodicity results in the unit cell exhibiting dimensions of 60 by 40 by $5mm$, which is optimized for a 60% volume constraint as with the single component example. The optimized compliance value achieved is raised due to the enforcement of periodicity to a value of $0.85Nmm$.

The application of simple periodicity within a single component structure, as seen in Fig. 5(b), does not realistically model assembly conditions. The premise of periodic design is the separate fabrication of unit cells and assembly into a macro-structure; thus, multi-component assembly should be incorporated into the finite element model and optimization process. The same concept of a cantilever case study may be extended to a multi-component cantilever system consisting of two components connected via a series of joints in an overlapping region. Simultaneous optimization of the components and interface joint region may then be applied, for a prescribed component volume and joint quantity. An example of this premise may be seen in the third result set of Fig. 5(c), for a two-component steel cantilever beam system connected via eight joints. The component dimensions are both 80 by 40 by $5mm$, meshed with 84 by 42 by 4 elements, with an overlapping region of 40 by $40mm$, which is joined via $2.15mm$ aluminum rivets modeled as a joint sizing of $m = n = 2$ and $\Delta_c^e = 2$. The total length of the model remains $120mm$ as in the single component model, with a new component volume constraint of 45% such that the total material volume is equivalent between the single and two-component models. As may be seen, the addition of joint interfacing and separation of the system into two-components increases the optimized compliance value to $0.95Nmm$. Furthermore, periodicity may be enforced in the multi-component optimization, as seen in the final result set of Fig. 5(d) for a 2 by 1 multi-component periodic. In this scenario, the optimized compliance value is increased both by the multi-component design and the periodicity to a value of $1.14Nmm$. The addition of each new fabrication requirement to the optimization model increases the final compliance value, highlighting the current disparity between most topology optimization literature and real engineering designs.

5.2 Simply supported bridge

Periodic topology optimization is a significantly smaller field than single component topology optimization and as such there is no universal case study within the literature. However, a commonly considered case is that of a two-dimensional simply supported bridge structure under a central loading (Huang and Xie 2008). The nature of periodic topology optimization then allows for any arbitrary m by n periodicity to be applied translationally to the bridge structure. An example of this premise may be seen in Fig. 6,

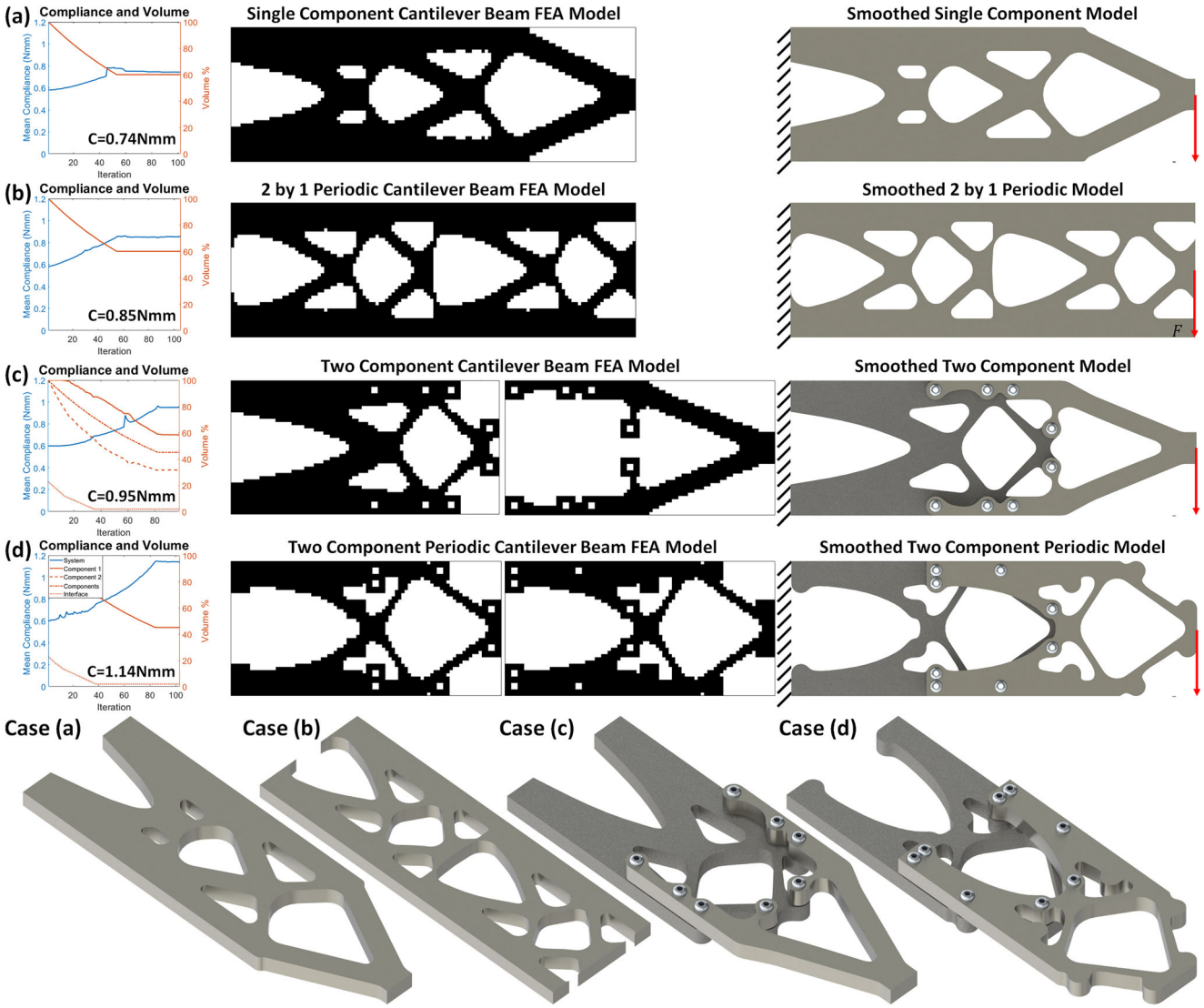

Fig. 5 Topology optimization of single and multi-component cantilever structures

which juxtaposes single component topology optimization with a 4 *by* 1 translational periodic topology optimization for a volume constraint of 50%. The bridge dimensions are 400 *by* 100 *by* 20*mm*, modeled with a steel material and a central 1000*N* load. Each unit cell in the periodic design is 100 *by* 100 *by* 20*mm*. The single component topology optimization achieves an optimized compliance of 2.8*Nmm* and the 4 *by* 1 periodic a 4.8*Nmm* compliance, an increase of approximately 70% in the periodic topology, as seen in Fig. 6.

Each of the concepts in the previous examples may be utilized to extend the premise of a simple case study topology to that of a periodic multi-component assembly. A similar bridge topology to the variant seen in Fig. 6 may be formed consisting of multiple periodic components. Due to assembly and interfacing requirements there must exist overlapping regions between sub-components, connected via interfacing joints. This may be achieved through a sandwich design of periodic plate components. An example of this premise may be seen in Fig. 7 for a 4 *by* 2 periodic bridge topology connected via a fully populated set of rivets (a), with the periodic unit cell seen on the right of the figure (b).

The following example results, in Figs. 8, 9, 10, 11, and 12, illustrate several optimized *m by n* periodic multi-component bridge topologies subjected to a central vertical loading of 1000*N*. The target component volume reduction is set to 50% with a joint volume criterion of 4 joints per overlapping interface. The dimensions of each of the steel plate components' cross sections are 100 *by* 100*mm* with a thickness of 5*mm* for the outer plates and 10*mm* for the inner plates. Each adjacent plate is separated within the cross-sectional plane by a 10 *by* 10*mm* spacing and a depth spacing of 1*mm*, such that a repeating periodic cell in the macro-topology has dimensions of 110 *by* 110

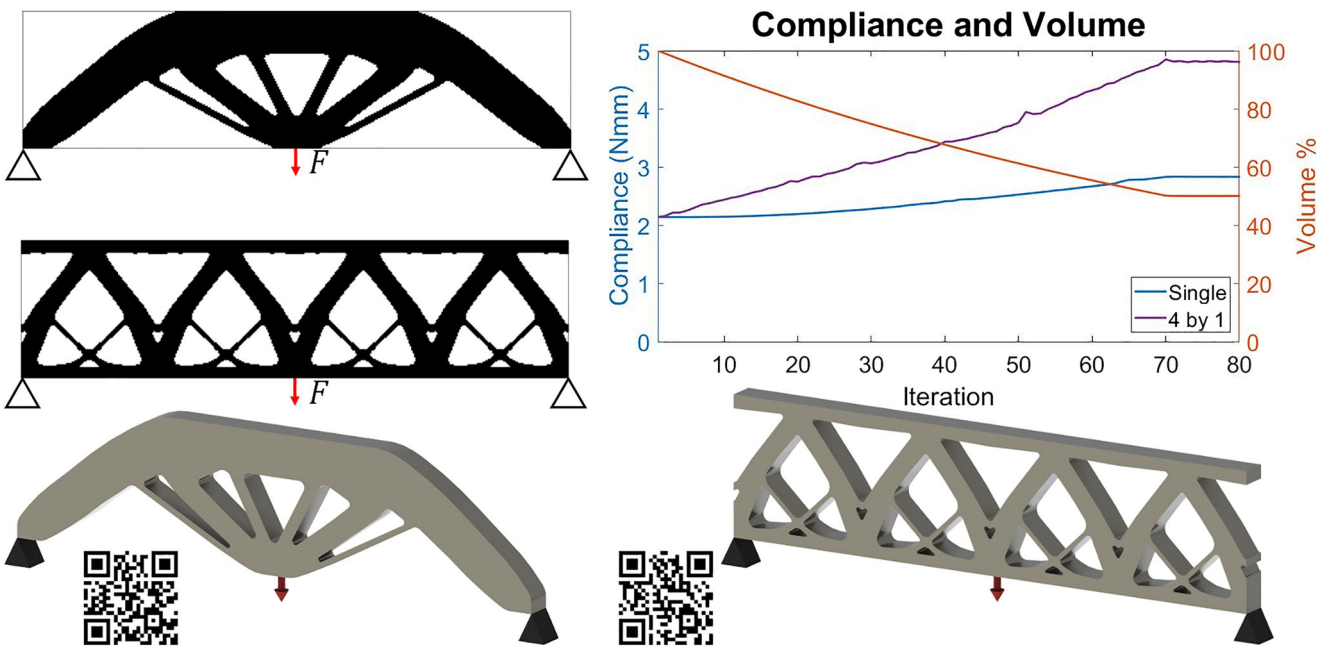

Fig. 6 Topology optimization of simply supported bridge structure for single component and 4 *by* 1 periodic

by 22*mm*. The joints are modeled as aluminum rivets with a 3.2*mm* shaft diameter and a 5.5*mm* head diameter. A 6*mm* separation between each rivet location is set to account for assembly conditions and to prevent contact between adjacent rivets, and this manifests as an $m = 3, n = 3$, and $\Delta_c^e = 3$ joint meshing, where a fixed grid is utilized with element cross-sections of 1 *by* 1*mm*. The evolutionary rate is set to 1% for component volume and the joint removal and addition rates are set to 2 and 1 respectively, per interface region. The convergence threshold is set to 0.001 and the filter radius is 5*mm*. Each of the optimizations begins with a fully populated design space of 100% component volume and 49 joints per interface region.

Figure 8 depicts a 2 *by* 1 optimized periodic topology achieving a final compliance value of 14.2*Nmm* from an initial value of 9.1*Nmm*, an increase of 56% in compliance for the 50% component volume reduction, and an interface volume reduction of over 90%. Figure 9 depicts the optimized result for a 5 *by* 1 periodic with an initial compliance value of 30.9*Nmm* and an optimized value of 126.2*Nmm*, an increase of 126%. Figure 10 depicts an optimized result for a two-dimensional periodicity of 4 *by* 2, in which an initial compliance value of 10.4*Nmm* is raised to 21.3*Nmm* for a compliance increase of 105%. The optimization seen in Fig. 11 for a 7 *by* 2 periodic depicts an initial compliance of 17.0*Nmm* raised to 44.7*Nmm*, an increase of 164%. A variety of results for other *m by n* periodicities may be found in Fig. 12, or in the accompanying data set (Thomas 2019).

The concept of multi-component periodic optimization may be extended to more complex periodic systems. This increase in complexity may include aspects such as a variety of unique periodic cells, three-dimensional optimization, self-interlocking components, multiple joint types within interface regions, or more complex unit cell geometry. An example of this premise may be seen in Fig. 13 in which

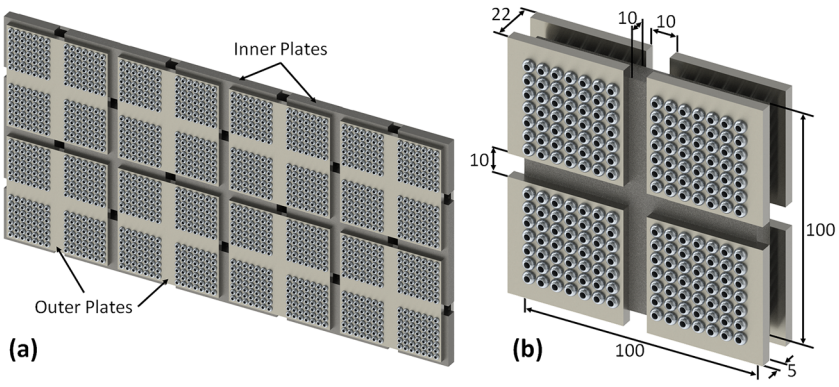

Fig. 7 4 *by* 2 multi-component periodic bridge topology example

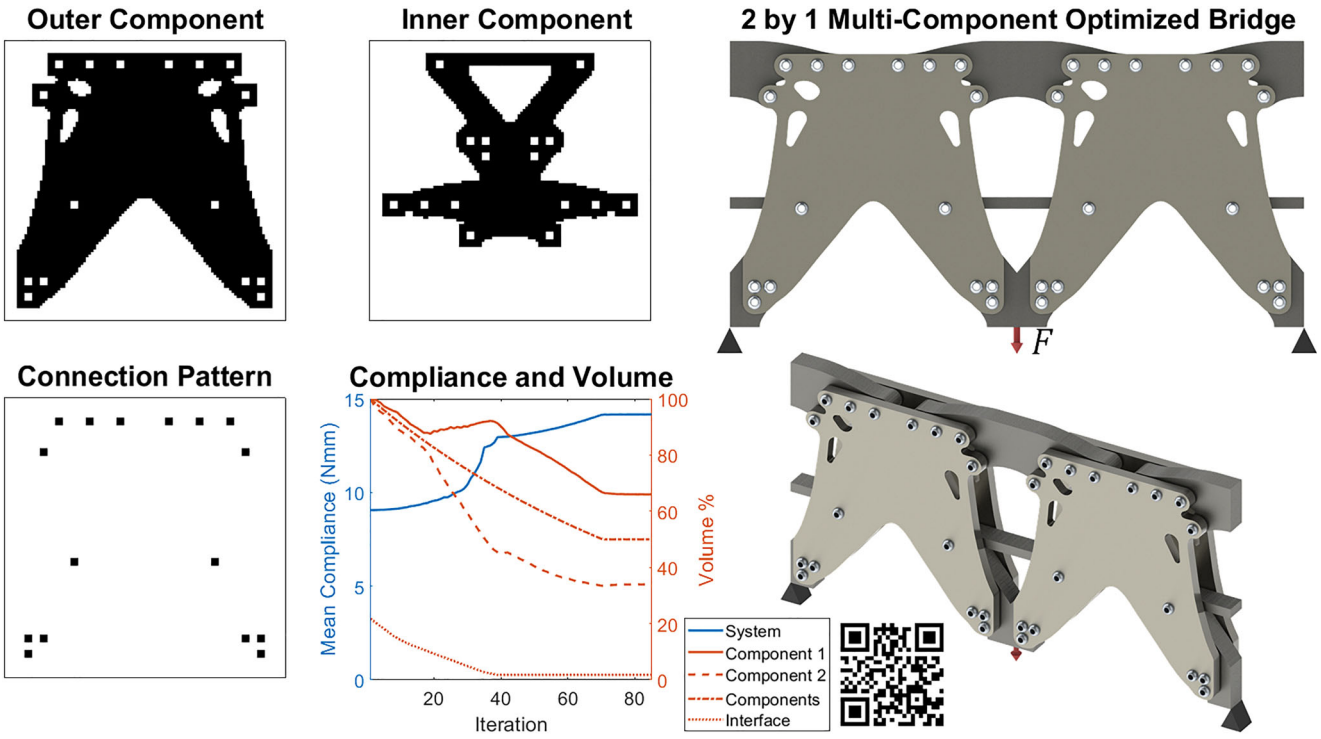

Fig. 8 2 *by* 1 multi-component periodic bridge topology optimization

two simply supported bridge structures, subjected to central loading, are formed via three-dimensionally optimized self-interlocking periodic components, connected via pin joints/bolts. As a result of the self-interlocking constraint between the periodic cells, the connection interface pattern optimization is restricted to a single quadrant of the periodic design, each interface reduced to 3 joint locations. The first example (a) depicts a 3 *by* 2 periodic topology in which the

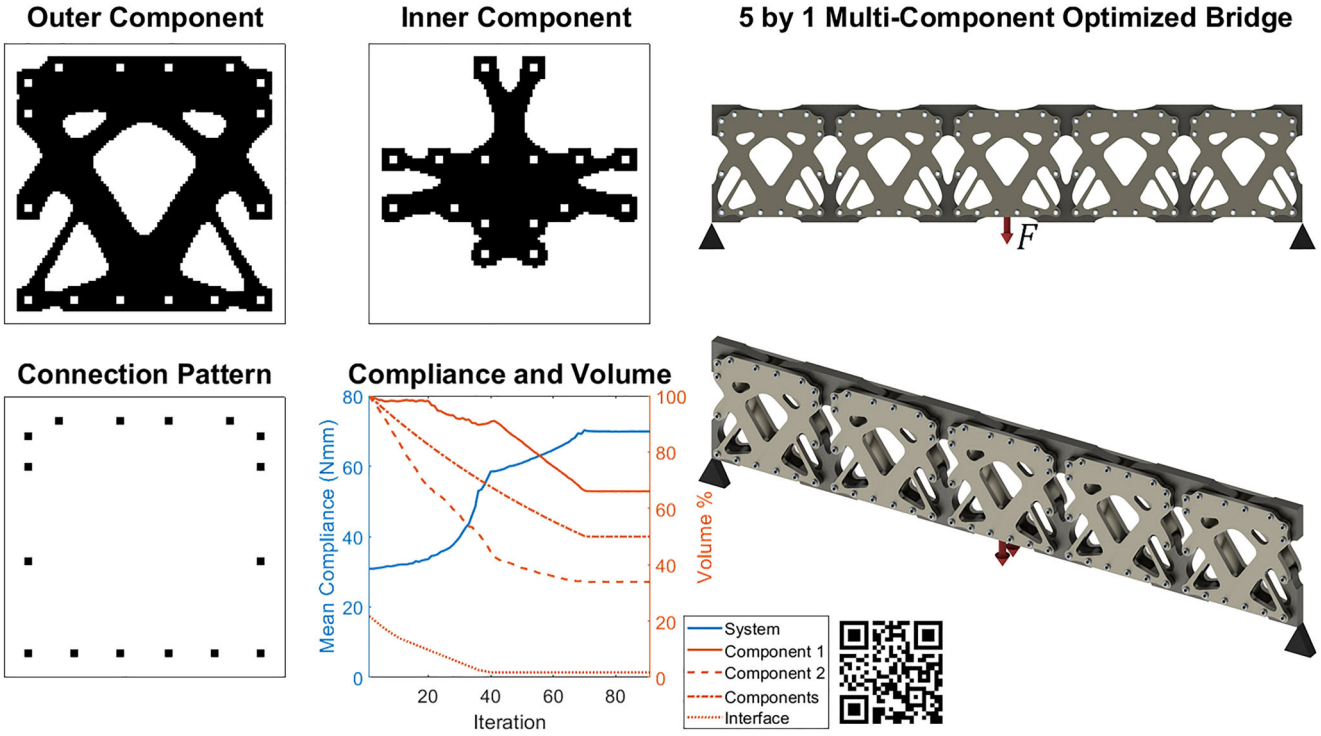

Fig. 9 5 *by* 1 multi-component periodic bridge topology optimization

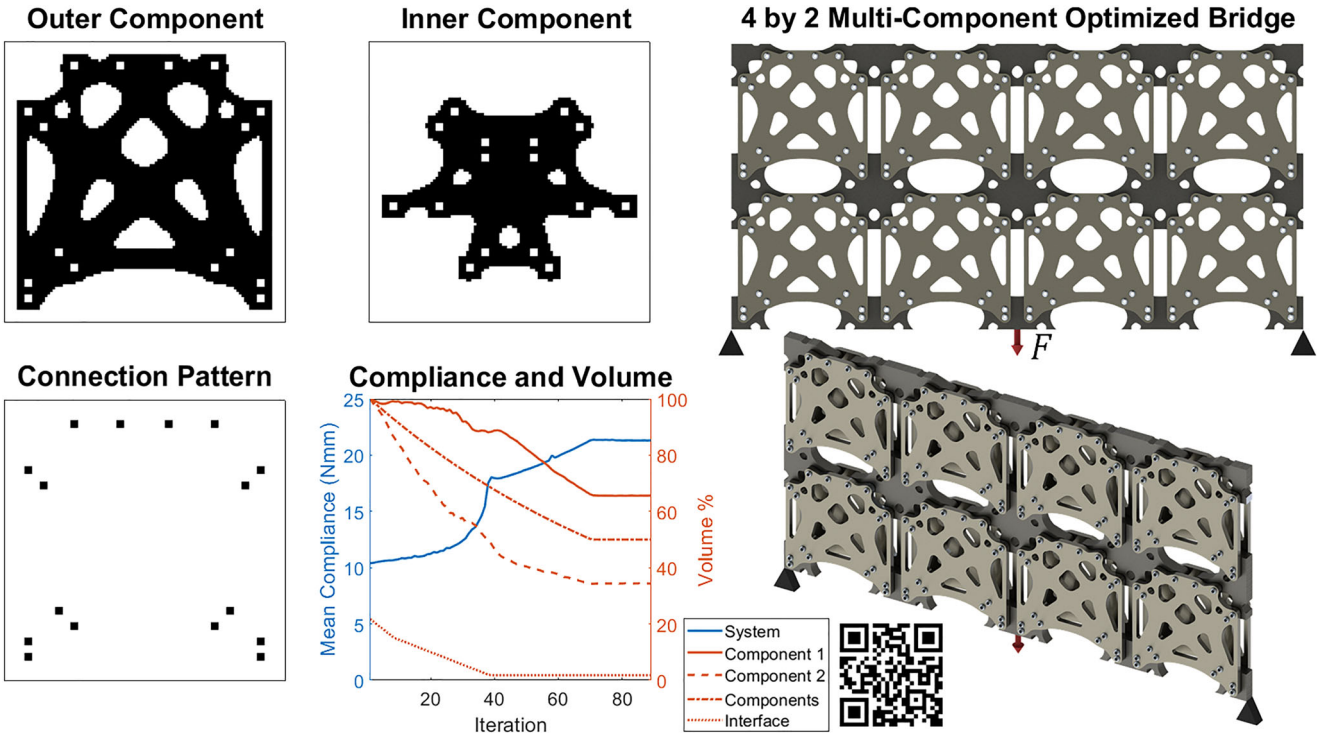

Fig. 10 4 *by* 2 multi-component periodic bridge topology optimization

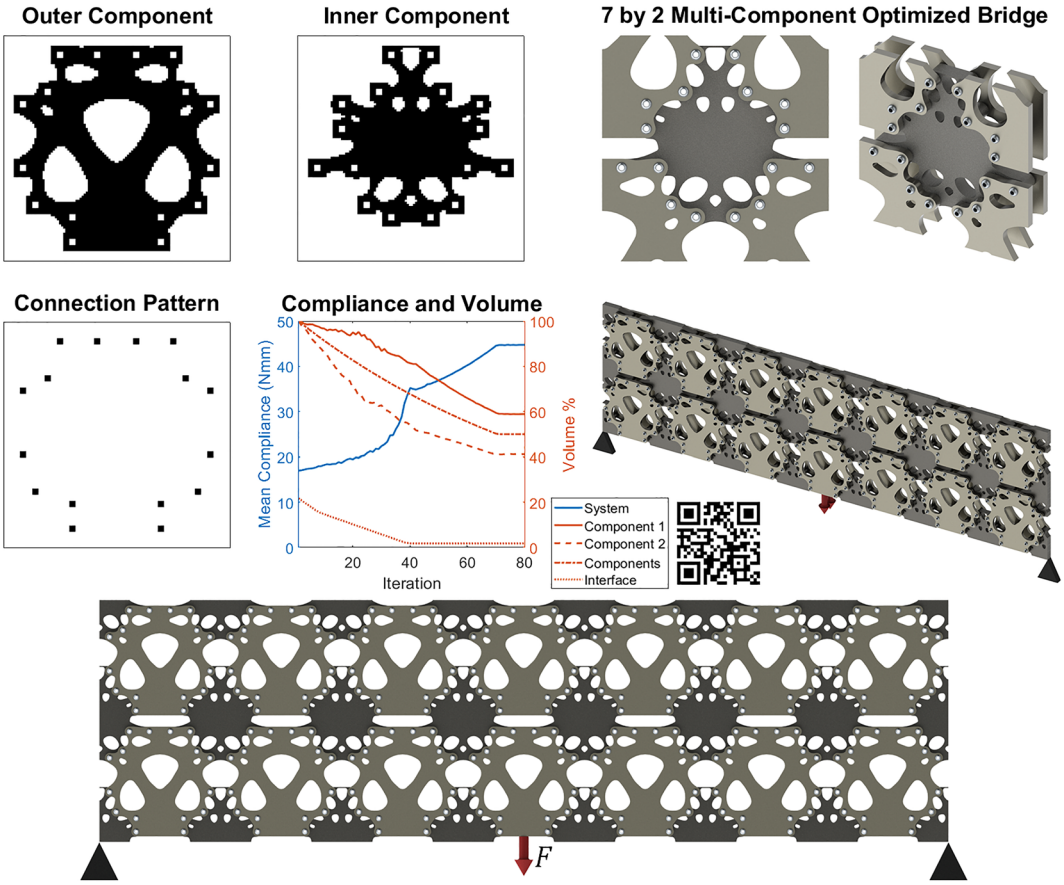

Fig. 11 7 *by* 2 multi-component periodic bridge topology optimization

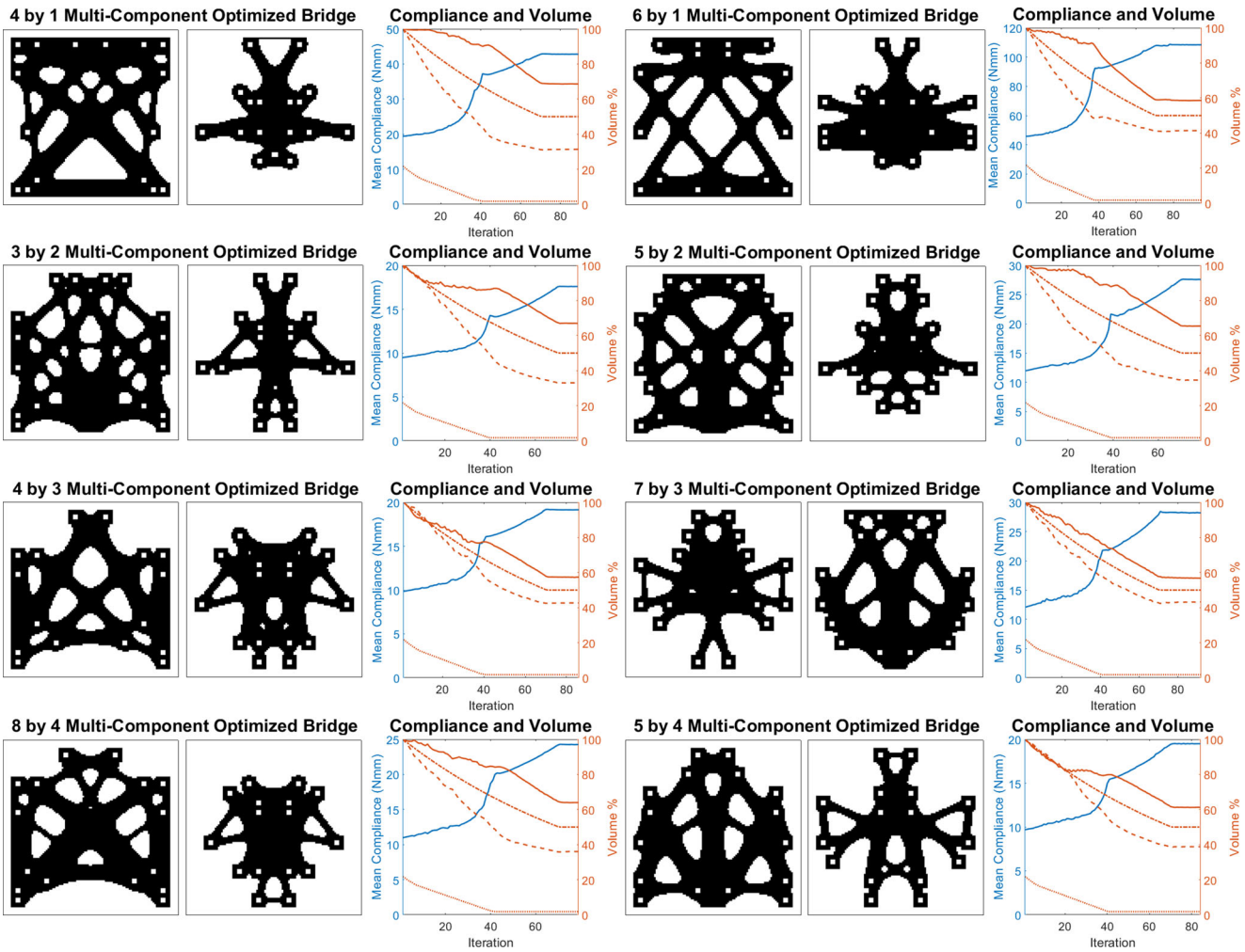

Fig. 12 Various multi-component periodic bridge topology optimization results

optimized output design exhibits a final compliance value of $7.5Nmm$, increased from the initial value of $4.2Nmm$. This equates to a 75% increase in compliance for a 60% reduction in component volume. The second example (b) depicts a 5 *by* 2 periodic with a significantly larger spacing between each periodic cell. The optimized design exhibits a final compliance value of $9.0Nmm$, raised from an initial value of $2.9Nmm$, an increase of 216% for a 75% component volume reduction.

In each of the depicted results for multi-component periodic optimization, the joint volume target is achieved relatively early in the optimization processes, as illustrated by the large compliance gains in the early iterations. The component topologies then stabilize around the ultimate joint locations, with a significant reduction in subsequent compliance gains per iteration. A disparity in the iterations required to reach the volume criterion in components and interfacing regions may be addressed through a reduction in joint removal rate or updating the joint interfacing every $n-th$ iteration. The evolutionary rate, joint removal and addition rates, number of joints, and volume criterion are user-assigned variables and may be chosen from a wide range of viable values.

5.3 Effects of initial joint discretization

Specification of appropriate joint type is a large contributing factor to the final optimized design. Various initial discretizations may be utilized, each corresponding to a specific joint type (sizing and spacing) desired by a design engineer. Figure 14 examines three different initial joint discretizations for a 3 *by* 1 multi-component periodic topology: (a) $3.2mm$ rivets with joint meshing of $m=3$, $n=3$, and $\Delta_c^e=3$; (b) $4.5mm$ rivets with a joint meshing of $m=4$, $n=4$, and $\Delta_c^e=4$; and (c) $5.5mm$ rivets with a joint meshing of $m=5$, $n=5$, and $\Delta_c^e=5$. The joints are modeled to have an equivalent cross-sectional area as the intended rivet type, despite the square cross-sectional geometry in the FEA model. Each of the modeled cases utilizes a different target joint constraint for each for the interface regions, such that

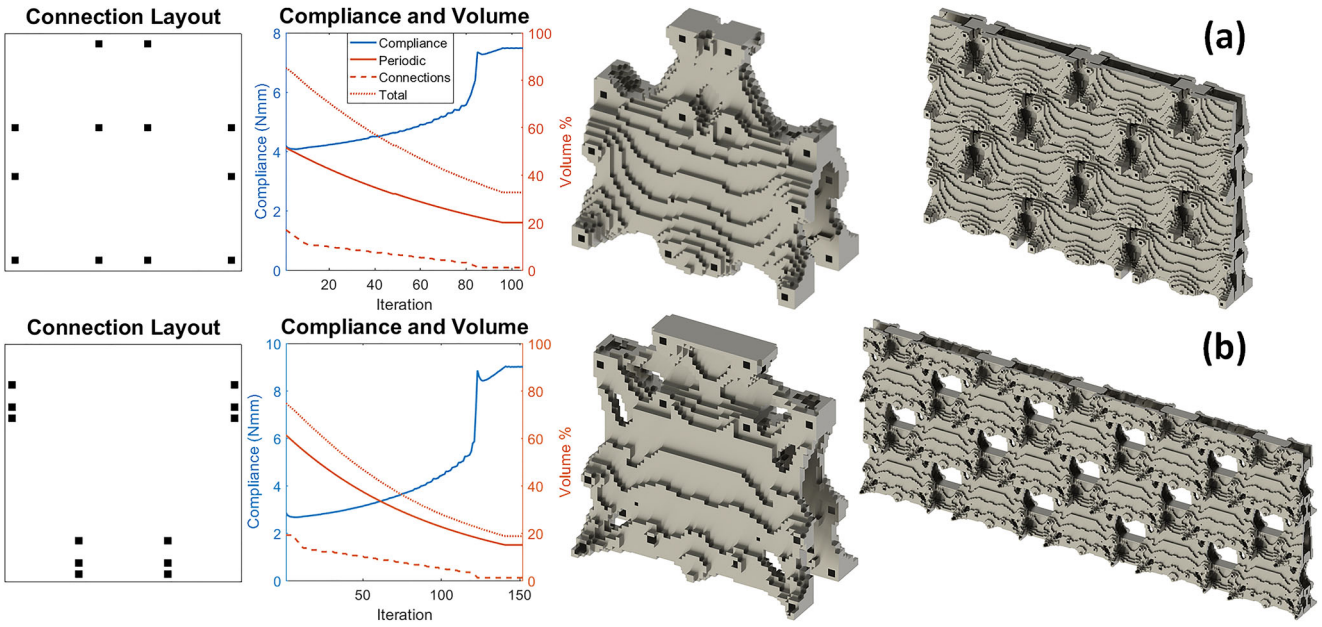

Fig. 13 3D self-interlocking multi-component periodic topology optimization

the total joint material volume in each case is approximately equivalent. As may be seen, (a) utilizing five 3 *by* 3 element joints for a total connection area of $45mm^2$ per interface achieved a final compliance value of $25.1Nmm$, (b) utilizing three 4 *by* 4 element joints for a total connection area of $48mm^2$ per interface achieved a final compliance value of $25.2Nmm$ and (c) utilizing two 5 *by* 5 element joints for a total connection area of $50mm^2$ per interface achieved a final compliance value of $29.1Nmm$. Despite a slightly lower total connective area, the larger number of connection points produced comparatively lower compliance values. This is primarily due to two factors: the requirement of excessive low-value material to surround large joint locations (to account for the rivet head sizing) and a reduction

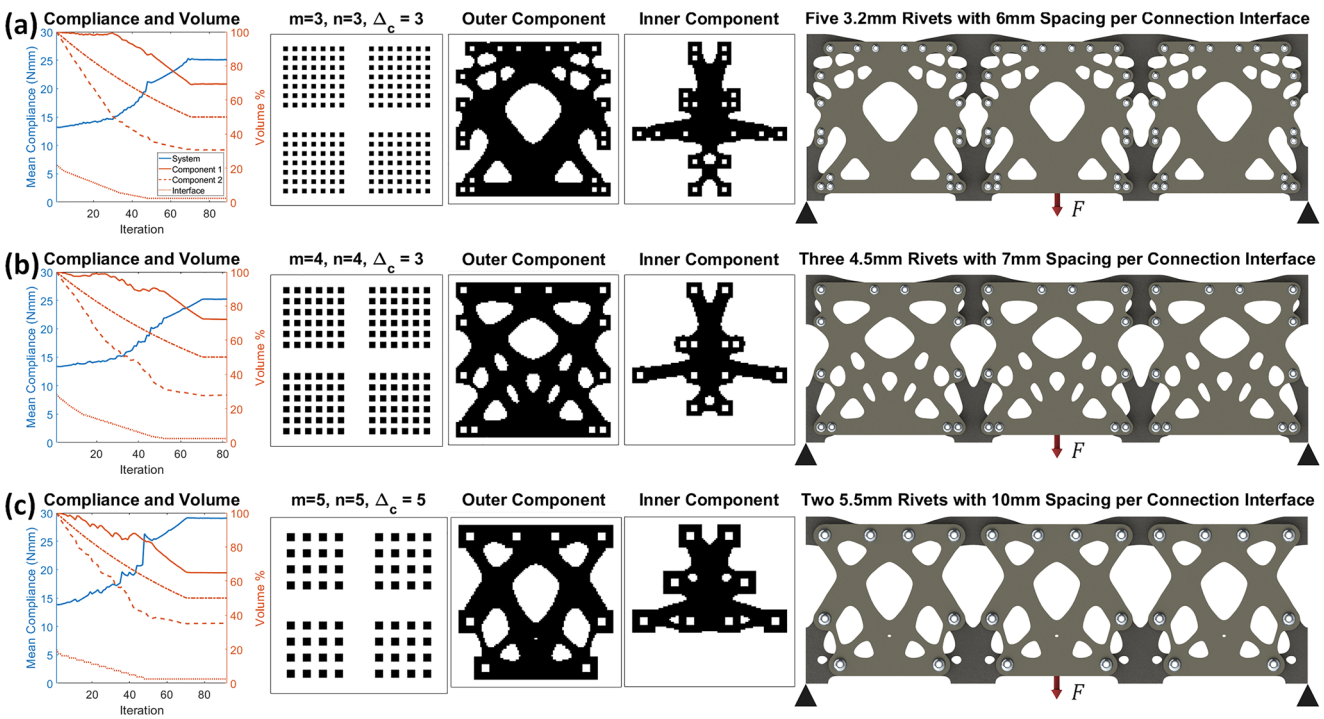

Fig. 14 3 *by* 1 multi-component periodic optimized designs for various initial discretizations

in geometric complexity with lower numbers of interface connection points.

5.4 Multi-criteria optimization example

Frequency-based topology optimization can be a volatile process for periodic multi-component structures, typically prone to geometric disconnections and poor convergence. To deal with these issues, it is often easiest to apply frequency optimization in conjunction with a more stable criterion such as stiffness. Figure 15 displays several optimization results for a 4 *by* 1 periodic fixed bridge structure subjected to two lateral loading cases. The multi-criteria optimization is conducted for minimization of mean compliance and maximization of the first natural frequency for a range of weighting factors, utilizing (10). As seen in Fig. 15, larger weighting factors produce stiffer topologies (lower compliance) but a lower first natural frequency, whereas the lower weighting factors produce less-stiff topologies but higher first frequencies. It is noted that the optimized designs vary both in periodic component and connective layout for the different weighting factors. Application of this process to engineering designs will allow a compromise between dynamic (natural frequency) and static (stiffness) criteria.

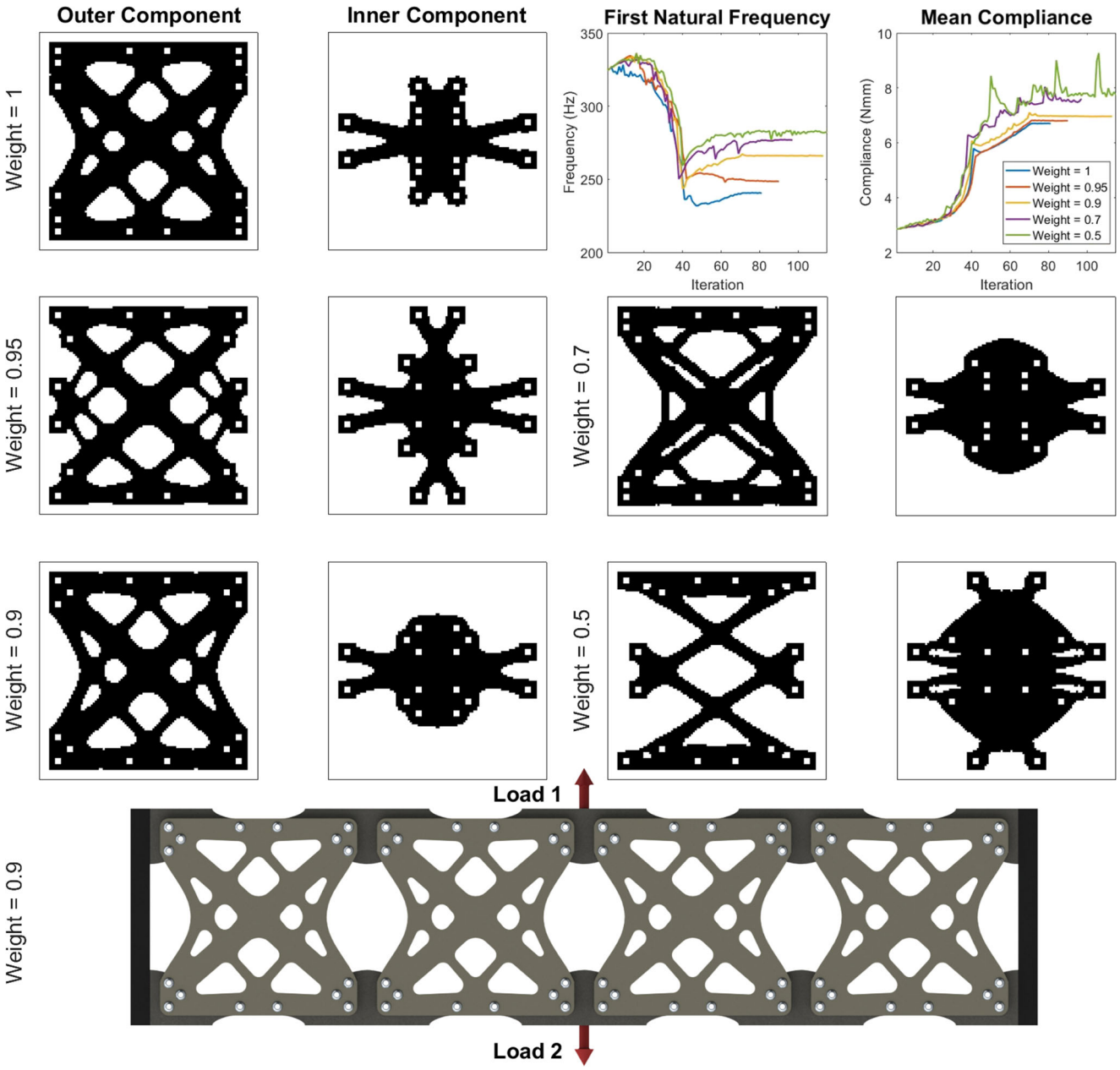

Fig. 15 Multi-criteria optimization for 4 *by* 1 periodic fixed bridge structure

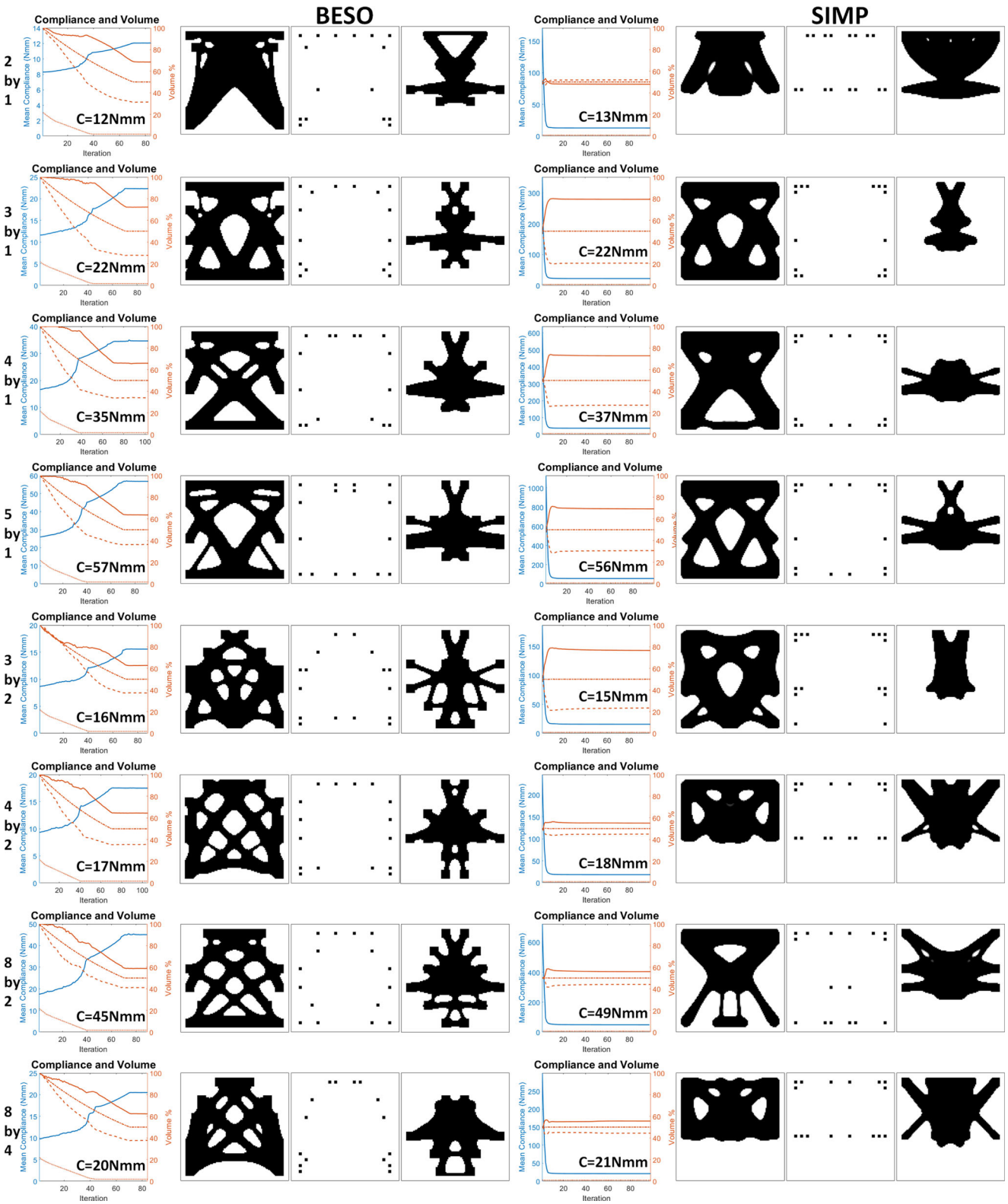

Fig. 16 BESO and SIMP comparison for spot-welded multi-component periodic bridge structures

5.5 Comparison of SIMP and BESO

The proposed methodology is not limited solely to BESO based applications; it is similarly applicable to SIMP, level-set, and other optimization procedures. As SIMP shares common similarities with the BESO methodology, it will be examined as a point of comparison. A standard power law scheme of $p = 3$ is adopted for material properties, a mesh-independent filter is utilized, and the topology updated with an optimality criterion of move limit $m = 0.2$.

The following optimized models, in Fig. 16, utilize spot-weld connections between component interfaces and are examined for a variety of periodicities; the joint discretization, component dimensions, and mesh are the same as for the examples in Figs. 8, 9, 10, 11, and 12. The spot weld connection is modeled as a material interface layer between each component, without any through-holes into the connecting components as was seen in the previous rivetted examples. The optimization processes for SIMP and BESO follow different search paths in the design domain and, as a result, arrive at different local optima designs. However, despite being visually different, they exhibit similar compliance values which indicates the viability of both algorithms to the application of periodic multi-component design.

The BESO results on average exhibit slightly lower compliances values, the best improvement being an 8.1% compliance reduction, and the worst comparison being a 1.4% compliance increase compared with the SIMP results achieved in Fig. 16. The performance discrepancy is likely due to the inclusion of some gray-material existing in the SIMP designs, or due to the SIMP designs converging too quickly and being locked in a local-minima, while the BESO translation of joints helps prevent the algorithm being locked in non-optimal designs. However, the SIMP formulation utilized was a basic OC method and may exhibit improved results from more sophisticated SIMP algorithms. As with most literature on the comparison between SIMP and BESO results, each algorithm brings its own pros and cons (Rozvany 2009; Huang and Xie 2010; Sigmund and Maute 2013; Xia et al. 2018). The comparative results illustrated in Fig. 16 produce little variation in optimized objective functions indicating the application of either method will yield acceptable results.

6 Concluding remarks

This study presents a topology optimization framework for the design of periodic multi-component structures. The coupled optimization of component topology with connective layout addresses real assembly issues faced in the engineering design not typically accounted for in single component topology optimization procedures. Application of periodic topology optimization enables fabrication of smaller identical components with optimized designs and joint layouts for large-scale structural systems, significantly reducing design complexity and manufacturing cost as well as easing assembly/packing/transport requirements. A number of examples are provided to demonstrate the effectiveness of the proposed topology optimization procedure for periodic multi-component systems, with stiffness and frequency criteria, and is shown to be applicable to BESO and SIMP methodologies.

Acknowledgements The funding support from Australian Research Council (ARC) through Discovery scheme (DP190103752) is acknowledged. The first author is a recipient of Australian Government Research Training Program (RTP) Scholarship.

Compliance with ethical standards

Conflict of interest The authors declare that they have no conflict of interest.

Replication of results An accompanying data set may be found in the reference material. The dataset includes a variety of sample topologies and sample BESO optimization code utilizing the methodology detailed within this study (Thomas 2019).

References

Allaire G, Jouve F, Toader AM (2004) Structural optimization using sensitivity analysis and a level-set method. J Comput Phys 194(1):363–393
Bendsøe MP (2009) Topology optimization. Springer, Berlin
Bendsøe MP, Kikuchi N (1988) Generating optimal topologies in structural design using a homogenization method. Comput Methods Appl Mech Eng 71(2):197–224
Bendsøe MP, Sigmund O (1995) Optimization of structural topology, shape, and material, vol 414. Springer, Berlin
Bendsøe MP, Sigmund O (1999) Material interpolation schemes in topology optimization. Arch Appl Mech 69(9-10):635–654
Bourdin B (2001) Filters in topology optimization. Int J Numer Methods Eng 50(9):2143–2158
Chen Y, Zhou S, Li Q (2010) Multiobjective topology optimization for finite periodic structures. Comput Struct 88(11-12):806–811
Chickermane H, Gea H (1997) Design of multi-component structural systems for optimal layout topology and joint locations. Eng Comput 13(4):235–243
Chirehdast M, Jiang T (1996) Optimal design of spot-weld and adhesive bond pattern. Tech. rep., SAE Technical Paper
Cook RD et al (2007) Concepts and applications of finite element analysis. Wiley, New York
Hassani B, Hinton E (1998) A review of homogenization and topology optimization I—homogenization theory for media with periodic structure. Comput Struct 69(6):707–717
Hoang VN, Jang GW (2017) Topology optimization using moving morphable bars for versatile thickness control. Comput Methods Appl Mech Eng 317:153–173
Huang X, Xie M (2010) Evolutionary topology optimization of continuum structures: methods and applications. Wiley, New York
Huang X, Xie Y (2007) Convergent and mesh-independent solutions for the bi-directional evolutionary structural optimization method. Finite Elem Anal Des 43(14):1039–1049

Huang X, Xie Y (2008) Optimal design of periodic structures using evolutionary topology optimization. Struct Multidiscip Optim 36(6):597–606
Huang X, Xie YM (2010) A further review of ESO type methods for topology optimization. Struct Multidiscip Optim 41(5):671–683
Huang X, Zuo Z, Xie Y (2010) Evolutionary topological optimization of vibrating continuum structures for natural frequencies. Comput Struct 88(5-6):357–364
Jiang T, Chirehdast M (1997) A systems approach to structural topology optimization: designing optimal connections. J Mech Des 119(1):40–47
Lencus A, Querin OM, Steven GP, Xie Y (2002) Aircraft wing design automation with ESO and GESO. Int J Vehicle Des 28(4):356–369
Li Q, Steven GP, Querin OM, Xie Y (1999) Shape and topology design for heat conduction by evolutionary structural optimization. Int J Heat Mass Transf 42(17):3361–3371
Li Q, Steven G, Xie Y (2001) A simple checkerboard suppression algorithm for evolutionary structural optimization. Struct Multidiscip Optim 22(3):230–239
Li Q, Steven GP, Xie Y (2001) Evolutionary structural optimization for connection topology design of multi-component systems. Eng Comput 18(3/4):460–479
Liu J, Ma Y (2016) A survey of manufacturing oriented topology optimization methods. Adv Eng Softw 100:161–175
Liu J, Ma YS (2015) 3D level-set topology optimization: a machining feature-based approach. Struct Multidiscipl Optim 52(3):563–582
Liu P, Kang Z (2018) Integrated topology optimization of multi-component structures considering connecting interface behavior. Comput Methods Appl Mech Eng 341:851–887
Ma ZD, Kikuchi N, Hagiwara I (1993) Structural topology and shape optimization for a frequency response problem. Comput Mech 13(3):157–174
Menassa R, DeVries W (1991) Optimization methods applied to selecting support positions in fixture design. J Eng Ind 113(4):412–418
Menassa RJ, DeVries WR (1989) Locating point synthesis in fixture design. CIRP Ann 38(1):165–169
Munk DJ, Vio GA, Steven GP (2017) A bi-directional evolutionary structural optimisation algorithm with an added connectivity constraint. Finite Elem Anal Des 131:25–42
Pedersen NL (2000) Maximization of eigenvalues using topology optimization. Struct Multidiscipl Optim 20(1):2–11
Qian Z, Ananthasuresh G (2004) Optimal embedding of rigid objects in the topology design of structures. Mech Based Design Struct Mach 32(2):165–193
Rodrigues H, Guedes JM, Bendsoe M (2002) Hierarchical optimization of material and structure. Struct Multidiscip Optim 24(1):1–10
Rong J, Xie Y, Yang X, Liang Q (2000) Topology optimization of structures under dynamic response constraints. J Sound Vib 234(2):177–189
Rozvany GI (2009) A critical review of established methods of structural topology optimization. Struct Multidiscipl Optim 37(3):217–237
Schevenels M, Lazarov BS, Sigmund O (2011) Robust topology optimization accounting for spatially varying manufacturing errors. Comput Methods Appl Mech Eng 200(49-52):3613–3627
Shu L, Wang MY, Fang Z, Ma Z, Wei P (2011) Level set based structural topology optimization for minimizing frequency response. J Sound Vib 330(24):5820–5834
Sigmund O (1994) Materials with prescribed constitutive parameters: an inverse homogenization problem. Int J Solids Struct 31(17):2313–2329
Sigmund O (2001) A 99 line topology optimization code written in Matlab. Struct Multidiscipl Optim 21(2):120–127
Sigmund O (2007) Morphology-based black and white filters for topology optimization. Struct Multidiscip Optim 33(4-5):401–424
Sigmund O (2009) Manufacturing tolerant topology optimization. Acta Mech Sinica 25(2):227–239
Sigmund O, Maute K (2013) Topology optimization approaches. Struct Multidiscip Optim 48(6):1031–1055
Sigmund O, Petersson J (1998) Numerical instabilities in topology optimization: a survey on procedures dealing with checkerboards, mesh-dependencies and local minima. Struct Optim 16(1):68–75
Tcherniak D (2002) Topology optimization of resonating structures using SIMP method. Int J Numer Methods Eng 54(11):1605–1622
Thomas S (2019) Topology optimization for periodic multi-component structures with stiffness criteria data set. Mendeley. https://doi.org/10.17632/xcxpbnywbc.1
van Dijk NP, Maute K, Langelaar M, Van Keulen F (2013) Level-set methods for structural topology optimization: a review. Struct Multidiscip Optim 48(3):437–472
Wang MY, Wang X, Guo D (2003) A level set method for structural topology optimization. Comput Methods Appl Mech Eng 192(1-2):227–246
Wang X, Long K, Hoang VN, Hu P (2018) An explicit optimization model for integrated layout design of planar multi-component systems using moving morphable bars. Comput Methods Appl Mech Eng 342:46–70
Xia L, Xia Q, Huang X, Xie YM (2018) Bi-directional evolutionary structural optimization on advanced structures and materials: a comprehensive review. Arch Comput Methods Eng 25(2):437–478
Xie Y, Steven G (1994) A simple approach to structural frequency optimization. Comput Struct 53(6):1487–1491
Xie Y, Steven G (1996) Evolutionary structural optimization for dynamic problems. Comput Struct 58(6):1067–1073
Xie Y, Zuo Z, Huang X, Tang J, Zhao B, Felicetti P (2011) Architecture and urban design through evolutionary structural optimisation algorithms. In: Proceedings of the International Symposium on Algorithmic Design for Architecture and Urban Design, vol 22
Xie YM, Steven GP (1993) A simple evolutionary procedure for structural optimization. Comput Struct 49(5):885–896
Xie YM, Steven GP (1997) Basic evolutionary structural optimization. In: Evolutionary structural optimization, Springer, pp 12–29
Xie YM, Zuo ZH, Huang X, Rong JH (2012) Convergence of topological patterns of optimal periodic structures under multiple scales. Struct Multidiscip Optim 46(1):41–50
Yang X, Xei Y, Steven G, Querin O (1999) Bidirectional evolutionary method for stiffness optimization. AIAA J 37(11):1483–1488
Yang X, Xie Y, Steven G, Querin O (1999) Topology optimization for frequencies using an evolutionary method. J Struct Eng 125(12):1432–1438
Zhang W, Sun S (2006) Scale-related topology optimization of cellular materials and structures. Int J Numer Methods Eng 68(9):993–1011
Zhang W, Xia L, Zhu J, Zhang Q (2011) Some recent advances in the integrated layout design of multicomponent systems. J Mech Des 133(10):104503
Zhou M, Rozvany G (2001) On the validity of ESO type methods in topology optimization. Struct Multidiscip Optim 21(1):80–83
Zhou M, Fleury R, Shyy YK, Thomas H, Brennan J (2002) Progress in topology optimization with manufacturing constraints. In: 9th AIAA/ISSMO Symposium on Multidisciplinary Analysis and Optimization, p 5614
Zhu JH, Zhang WH, Xia L (2016) Topology optimization in aircraft and aerospace structures design. Arch Comput Methods Eng 23(4):595–622
Zhu JH, Guo WJ, Zhang WH, Liu T (2017) Integrated layout and topology optimization design of multi-frame and multi-component fuselage structure systems. Struct Multidiscip Optim 56(1):21–45
Zuo Z (2009) Topology optimization of periodic structures. PhD Thesis RMIT